RSC Advances

RSCPublishing

COMMUNICATION

Cite this: *RSC Advances*, 2013, **3**, 2197

Received 26th July 2012,
Accepted 16th December 2012

DOI: 10.1039/c2ra21582a

www.rsc.org/advances

Preparation of heteropoly acid based amphiphilic salts supported by nano oxides and their catalytic performance in the nitration of aromatics†

Peng-cheng Wang, Kai Yao and Ming Lu*

A series of Keggin heteropoly acid anion based amphiphilic salts supported by nano oxides were synthesized and used as catalysts in the nitration of aromatic compounds with HNO_3. The reaction conditions in the nitration of toluene were optimized and both 92.6% conversion and good *para* selectivity (*ortho* : *para* = 1.09) were obtained.

Introduction

The electrophilic nitration of aromatics is a widely studied and useful reaction as it can obtain many organic intermediates that are required in large tonnages.[1,2] However, the classic mixed-acid nitration systems that industry still largely rely upon have many disadvantages, such as poor selectivity, notorious corrosion, over-nitration and an aqueous washing stage, which result in a waste inorganic acid stream that brings serious pollution.[3,4] With these environmental concerns, there is good scope for research towards finding green and eco-friendly catalysts for the regioselective nitration of aromatic compounds.

Polyoxometalates (POMs) or heteropoly acids (HPAs) possessing the Keggin structure are extensively studied as acid catalysts for many laboratorial and industrial processes.[5–8] Their application in nitration has also been reported.[9–11] Sato *et al.*[12,13] investigated the catalytic activity of HPAs in the vapor phase nitration of benzene, and indicated that the HPAs show extremely high activity in the form of their corresponding salts. However, bulk HPAs have a low thermal stability, low surface area ($2\ m^2\ g^{-1}$) and solubility in polar solvents. Recently, Heravi *et al.*[14] reported the regioselective nitration of phenol catalyzed by $H_{3+x}PMo_{12-x}V_xO_{40}$ in a heterogeneous system with different solvents and other parameters. Then, with the purpose of recovering HPAs, Kumar and Prasad[15] loaded the HPAs on silica and the nitration of phenol was also carried out.

More recently, the cation of phase transfer agents (PTAs) and the anion of HPAs were combined to synthesize a variety of amphiphilic catalysts, such as $[C_{18}TA]_5[PV_2Mo_{10}O_{40}]$,[16] $[(C_{18})_2DA]_3[PW_{12}O_{40}]$,[17] $[C_{18}TA]_4[H_2NaPW_{10}O_{36}]$[18] and $[Bmim]PMo_{12}O_{40}$.[19] The amphiphilic catalysts, assembled at the interface of emulsion droplets, could dramatically increase the total interface area. However, the demulsification process for catalyst recovery was often challenging in a large-scale unit.

Here, in order to develop new methods for the electrophilic nitration of aromatics with heteropoly acids, we prepared a series of nano material supported HPA-functionalized hybrid materials which exhibited the Keggin structure and had amphiphilic properties. Compared with the non-supported [bmim cation–heteropoly anion] complex, the distribution of the complex on a high surface area carrier was helpful to exhibit their catalytic effect while keeping a good emulsification of the reaction mixture.[19] Unlike other amphiphilic catalysts with longer chains where demulsification was needed for recycling, the supported catalysts were also easier to recover.

Experiments

Supported $[Bmim]_x$PAs were prepared by a co-precipitation method. One gram of the carrier (SiO_2, Al_2O_3, or TiO_2) was dispersed in 50 mL deionized water, and [Bmim]Br (0.029–0.175 g) was added dropwise to the slurry and stirred for 1 h. Then, 30 mL of the aqueous solution of HPA (0.081–0.486 g) was added dropwise. The resulting slurry was stirred for 2 h at room temperature, and the solid product was separated by filtration, washed with deionized water, and then dried at 100 °C for 12 h. The SiO_2-supported $[Bmim]_3PW_{12}O_{40}$ catalyst was denoted as Si–PW. Si–SiW, Si–PMo, Al–PW and Ti–PW stand for $[Bmim]_4SiW_{12}O_{40}$–SiO_2, $[Bmim]_3PMo_{12}O_{40}$–SiO_2, $[Bmim]_3PW_{12}O_{40}$–Al_2O_3 and $[Bmim]_3PW_{12}O_{40}$–TiO_2 respectively. Characterization methods are listed in the supplementary data.†

In a typical aromatic nitration process, to a vigorously stirred mixture of a given amount of catalyst and substrate (10 mL, 0.08mol), 67% nitric acid (1.05 equiv., 6mL) was added dropwise at room temperature. The reaction was warmed up to a higher

---

School of Chemical Engineering, Nanjing University of science and technology, Xiaolingwei 200, Nanjing, Jiangsu Province, China.
E-mail: luming@mail.njust.edu.cn; Fax: +86 25 84315514; Tel: +86 25 84315030

† Electronic supplementary information (ESI) available. See DOI: 10.1039/c2ra21582a

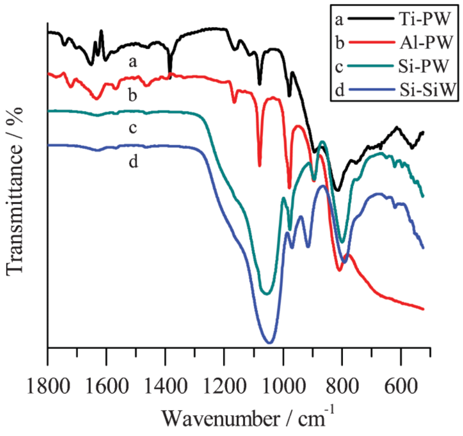

Fig. 1 FT-IR spectra of supported amphiphilic catalysts.

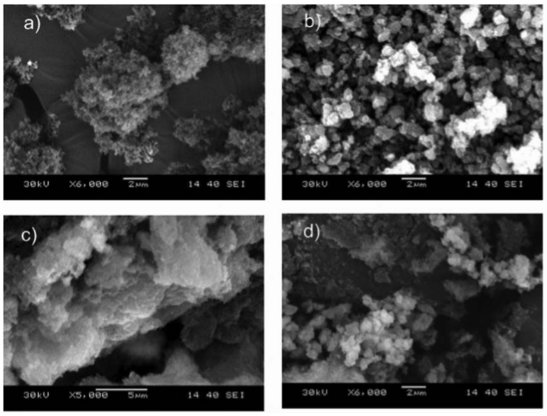

Fig. 2 SEM images of different catalysts. (a) Nano SiO_2; (b) Si–PW; (c) Ti–PW (d) Al–PW.

temperature, as indicated in Table 3. After 3 h, the solution was collected by filtration at negative pressure. The organic phase was isolated and washed with saturated sodium bicarbonate (5 mL), water (5 mL × 3), and brine (5 mL), dried over Na_2SO_4, and analyzed by GC or LC.

Mononitro-products were predominant in this nitration system, so the yield in theory was approximately equal to the conversion in most conditions and we took conversion as the measurable indicator. If there were dinitro-products or oxidized products, they would be marked.

Results and discussion

The FT-IR spectra of the synthesized materials were carried out and Fig. 1 shows the FT-IR data of various carriers and amphiphilic salts. The IR spectrum of $[Bmim]_3PMo_{12}O_{40}$ has been reported in the literature,[20] so it is not listed here. As shown in Fig. 1, stretching regions that are characteristic of the Bmim cation (1100–1600 cm^{-1})[21] and Keggin anion (450–1100 cm^{-1})[22] are clearly exhibited. A more detailed comparison of the supported and unsupported complexes can be found in Table S1 in the supporting information.† According to the BET surface area test listed in Table 1, we speculated that the high surface area of SiO_2 is beneficial to the dispersion of amphiphilic salt units. The two prominent vibrations at 860 cm^{-1} (lines a–c) and 930 cm^{-1} (line d) indicate the difference between the $PW_{12}O_{40}{}^{3-}$ and $SiW_{12}O_{40}{}^{4-}$ anions. SEM images in Fig. 2 provide a visual characterization of the materials. The particle size of the pure nano SiO_2 carrier is about 10–30 nm, as shown in Fig. 2(a), and a surface area as high as 500 $m^2 g^{-1}$ is provided. When HPAs are loaded on the support, the particle size increases to 100–500 nm (Fig. 2b), while the surface area is reduced. This increment of particle size might be due to the coating of HPAs on SiO_2 and the assembly of each nano carrier. The surface area also shows a decreasing trend when increasing the amount of HPA. It may be expected that plugging of the active component in the pores of the support decreases the surface area, at least in the case of highly loaded catalysts. The nano Al_2O_3 and TiO_2 (with a surface area of 150 $m^2 g^{-1}$ and 100 $m^2 g^{-1}$ respectively) also show a significant similar increment in particle size during preparation.

In our preliminary investigation, the electrophilic nitration of toluene was carried out as the typical reaction. Various nano material supported Keggin HPA-functionalized hybrid materials are tested and listed in Table 1. Without any catalyst, the reaction gives only 9.2% conversion of mononitrotoluene (MNT) and an *ortho* to *para* ratio of 1.77 with 65% nitric acid. When the amphiphilic salt $[Bmim]_3PW_{12}O_{40}$ is added, both the conversion and selectivity are improved. However, due to the low surface area of HPAs themselves, this improvement is not remarkable. When

Table 1 Nitration of toluene with various amphiphilic salt catalysts[a]

Entry	Catalysts	BET surface area ($m^2 g^{-1}$)	Product distribution (%)			*ortho* : *para*	Conv. (%)
			ortho	*meta*	*para*		
1	—	—	61.6	3.6	34.8	1.77	9.2
2	[Bmim]PW	15	52.8	4.1	43.1	1.23	29.7
3[b]	Si–PW	300	51.5	4.1	44.4	1.16	66.4
4	Si–PW	280	50.1	4.0	45.9	1.09	92.6
5	Al–PW	105	48.8	4.1	47.1	1.04	67.5
6	Ti–PW	50	47.6	4.0	48.4	0.98	45.7
7	Si–PMo	283	54.2	4.4	40.4	1.34	83.1
8	Si–SiW	292	52.5	4.0	43.5	1.21	89.3

[a] Toluene (0.08mol), 67% nitric acid (1.05 equiv.), cat. 1.0g, 50 °C, 3 h. [b] Heteropoly acids were loaded on the SiO_2, without ionic liquids.

distributed on the surface of nano carriers, better results are observed. The larger the surface area is, the higher the conversion that can be obtained. The nano SiO_2 support exhibited a surface area up to 280–290 $m^2\ g^{-1}$ and gives conversions of more than 80%. However, selectivity does not follow this trend. The *ortho* to *para* ratio with nano Al_2O_3 and TiO_2 supported amphiphilic salts (entries 5 and 6, Table 1) is lower than that of the nano SiO_2 support. We conjecture that there might be an interaction between the electron-deficient metal oxide and the electron-rich toluene, which results in a special substitution. Different reaction results are obtained with different HPAs. As can be seen, although owning the lowest surface area among the SiO_2 supporters, the $PW_{12}O_{40}{}^{3-}$ anion performs better than two other Keggin anions in both conversion and selectivity (entries 7 and 8, Table 1). Under the same nitration conditions, the catalytic activity follows the order $PW_{12}O_{40}{}^{3-}$ > $SiW_{12}O_{40}{}^{4-}$ > $PMo_{12}O_{40}{}^{3-}$. This trend is consistent with their acid strength, recorded by Yu and Liu.[23] Therefore, acid strength is another important factor besides surface area. The loading amount and the proportion of exposed heteropoly acid (single site) and the bulk structure (agglomerated sites) shall be taken into consideration to make an exact comparison of the activity among the samples. Then the activity site on surface could be determined by XPS. With conversion during a period of time, the turnover frequency (TOF) could be calculated, which would be considered as a factor to compare the activity among various samples. Our further work will focus on this area.

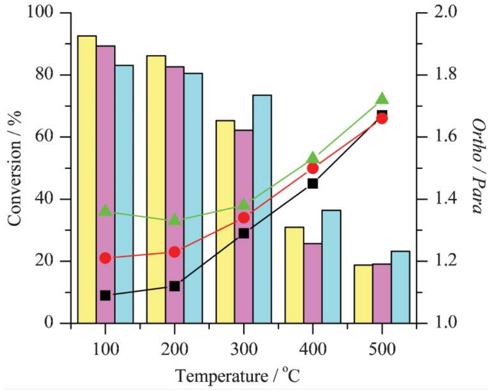

Fig. 3 Catalytic performance of supported amphiphilic salts calcinated at different temperatures. (🟨) Conversion of Si–PW; (🟪) conversion of Si–SiW; (🟦) conversion of Si–PMo; (■) selectivity of Si–PW; (•) selectivity of Si–SiW; (▲) selectivity of Si–PMo.

The influence of the loading amount was then investigated in the range 0–40 wt.% and the results are shown in Table 2. A maximum activity is observed at a loading of 10 wt.%, with the efficient formation of MNT at a conversion of 92.6%. The excellent activity as well as the selectivity of the catalyst may be due to the high surface area and well dispersed nature of amphiphilic materials loaded on silica. At lower loading, despite the high dispersion of the catalyst, the surface of the carrier is not fully covered. On the other hand, when the loading amount is over 10

Table 2 Loading amount of $[Bmim]_3PW_{12}O_{40}$ on SiO_2 in the nitration of toluene[a]

			Product distribution (%)				
Entry	Loading amount (wt.%)	BET surface area ($m^2\ g^{-1}$)	*ortho*	*meta*	*para*	*ortho* : *para*	Conv. (%)
1	0	500	61.6	3.6	34.8	1.77	9.2
2	5	410	51.5	3.9	44.6	1.15	59.3
3	10	280	50.1	4.0	45.9	1.09	92.6
4	20	190	50.7	3.9	48.4	1.05	86.4
5	40	110	48.9	4.1	47.0	1.04	75.9

[a] Toluene (0.08mol), 67% nitric acid (1.05 equiv.), cat. 1.0g, 50 °C, 3 h.

Table 3 Nitration of toluene under different reaction conditions

				Product distribution (%)				
Entry	Catalyst (g)[a]	*T* (°C)	Time (h)	*ortho*	*meta*	*para*	*ortho* : *para*	Conv. (%)
1	0.5	50	3.0	52.6	4.2	43.2	1.22	80.1
2	**1.0**	**50**	**3.0**	**50.1**	**4.0**	**45.9**	**1.09**	**92.6**
3	1.5	50	3.0	49.3	4.6	46.1	1.07	94.3
4	1.0	25	3.0	50.2	4.2	45.6	1.10	26.3
5	1.0	70	3.0	50.2	4.0	45.8	1.10	93.1[b]
6	1.0	50	4.0	50.0	4.1	45.9	1.09	95.2
7	1.0	50	4.5	49.3	4.6	46.1	1.07	95.8
8[c]	1.0	50	3.0	51.1	4.0	44.9	1.14	34.4
9[d]	1.0	50	3.0	49.2	4.0	46.8	1.05	97.8[b]

[a] Amount of catalyst Si–PW. [b] Over-nitrated products were found in GC. [c] 30% nitric acid was used. [d] 98% nitric acid was used.

Table 4 Selectivity on nitration of various substituted aromatics with Si–PW[a]

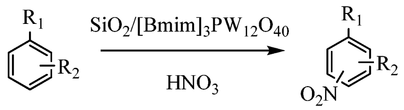

		Product distribution (%)				
Entry	Substrate	*2/6-*	*3/5-*	*4-*	Selectivity (*ortho* : *para*)	Conv. (%)
1	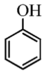	82.3	—	17.7	4.65	99.5
2	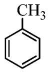	50.1	4.0	45.9	1.09	92.6
3	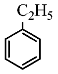	32.9	4.3	62.8	0.52	96.6
4	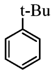	15.2	4.6	80.2	0.19	99.0
5	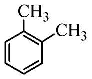	—	26.2	72.1	0.36[b]	100[c]
6	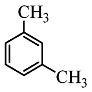	8.7	—	90.2	0.1	100[c]
7	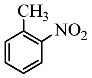	28.5		71.5	0.4	67.8
8	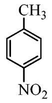	100	—	—	—	61.1
9	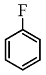	13.9	1.7	84.4	0.16	89.3
10	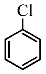	22.5	0.8	76.7	0.29	72.6
11	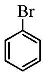	20.9	0.9	78.2	0.27	74.2
12	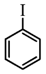	29.2	0.6	70.2	0.42	80.9
13	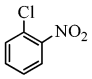	—	—	—	—	<1
14	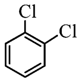	9.8		90.2	0.11	5.2

Table 4 (*Continued*)

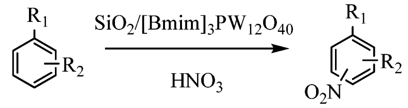

		Product distribution (%)				
Entry	Substrate	*2/6-*	*3/5-*	*4-*	Selectivity (*ortho* : *para*)	Conv. (%)
15	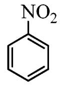	8.8	90.2	1.0	0.1[d]	12.3

[a] Aromatic (0.08mol), 67% nitric acid (1.05 equiv.), Si–PW 1.0 g, 50 °C, 3 h. [b] Ratio of 3-/4-. [c] Some *o*- and *m*- xylene is over-nitrated or oxidized [d] Ratio of 2-/4-.

wt.%, conversion will gradually decease, but no obvious change in the selectivity is observed. This can be attributed to the formation of bulk $[Bmim]_3PW_{12}O_{40}$ on the support surface. The surface area will reduce significantly because of agglomeration and the bulk itself, which results in fewer opportunities for contact between the catalysts and substrates.

The catalytic activity and thermal stability of different amphiphilic salts were also monitored, which allowed us to determine the stability of the compound. The effect of thermal treatment on the amphiphilic salts by thermogravimetric analysis and IR experiments has been reported by Rao *et al.*[20] In their work, there was a sharp loss of weight at about 400 °C, which suggests that the organic part (Bmim cation) begins to decompose. Then, the complete collapse of the Keggin structure to form a metal oxide phase was observed at 600 °C in TGA. As can be seen in Fig. 3, the conversion and selectivity of supported amphiphilic salts shows only a small drop after calcination at 200 °C. For $PW_{12}O_{40}^{3-}$ and $SiW_{12}O_{40}^{4-}$ structure salts, this drop becomes more serious when the calcination temperature reaches 300 °C, while the phenomenon occurs at 400 °C for $PMo_{12}O_{40}^{3-}$. This is closely related to the thermal stability of their Keggin structure. Although the Bmim cation does not strongly decompose at 300 °C, $PW_{12}O_{40}^{3-}$ and $SiW_{12}O_{40}^{4-}$ can not be sustained and will lose their secondary structure at this temperature. This problem will become more serious with the decomposition of the organic part when calcinated at 400 °C. The $PMo_{12}O_{40}^{3-}$ ion suffers both transformations mentioned above at 400 °C. For all three supported materials, most structures and the catalytic activity will be destroyed above 500 °C.

Several reaction factors are optimized, as shown in Table 3. It can be found that both conversion and selectivity increase with increasing amount of catalyst, yet this improvement becomes inconspicuous when the amount is over 1.0 g. A higher temperature gives a higher conversion. On the other hand, more byproducts such as dinitrotoluene are also generated. The reaction time has little influence on the selectivity and slow increments in conversion are witnessed when it is prolonged to 5 h. The nitrification strength relates to the concentration of nitronium ions (NO_2^+), which is the real electrophilic species in nitration. However, because its concentration is too low and even below the limits of spectroscopic determination in solution, this strength is usually defined as the effective concentration of nitric acid or sulfuric acid in waste acid in industry. Low nitration strength not only leads to a low conversion but also shows poor performance in selectivity. Although a high nitration strength improves both aspects, it brings unwanted byproducts (mainly oxidized products) at the same time, which means a waste of raw materials and a rise in economic cost.

Encouraged by the remarkable results obtained under the above reaction conditions, and in order to show the generality and scope of this new protocol, we applied this catalyst in the nitration of various substituted aromatics. The results obtained are summarized in Table 4. In the nitration of alkylbenzene, the same phenomenon is observed as in that of toluene: a higher conversion and *para*-selectivity than using mixed acid. A little difference is that the products of the *para*-position increase significantly with the steric effect of the substituted group. If there is another activated group such as –CH_3 on the benzene ring, all the substrates will be nitrated with some of them being over-nitrated or oxidized. When a nitro-group is introduced, the conversion will decrease sharply. The conversions of halobenzene are lower than that of toluene, since the electron induction caused by halogen atoms leads to a lower cloud density. The nitration of chlorobenzene demonstrates that the *para* position is more active than the *ortho* position, affording significantly higher *para*-selectivity with a 0.29 ratio of *ortho* to *para*. When another deactivation group is introduced, the conversion became worse, reaching no more than 6%. For some substituted aromatics that have no other products, their conversions are improved in this nitration system more or less. Another praiseworthy advantage of the system was that mononitro-products were predominant during the nitration process. Di-nitration and multi-nitration can only be seen with two highly activated substrates.

The recyclability of the catalytic system was also examined and the results with SiO_2–$[Bmim]_3PW_{12}O_{40}$ as an example are shown in Fig. 4. The untreated catalyst is directly used in the next step without purification, and the treated catalyst was heated at 100 °C for 2 h each time before being used. After four cycles, the

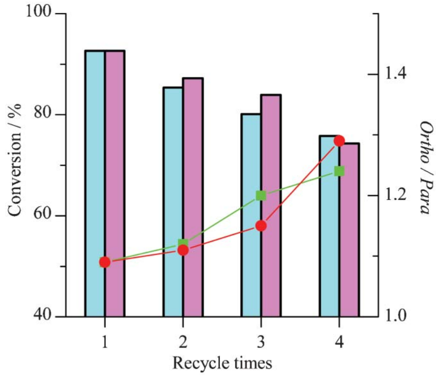

Fig. 4 Recycle times of treated and untreated Si–PW. (🟦) Conversion of untreated Si–PW; (🟪) conversion of treated Si–PW; (■) selectivity of untreated Si–PW; (•) selectivity of treated Si–PW.

conversion and *para*-selectivity of the untreated catalyst was decreased to only 75.8% and 1.24 respectively, indicating a good reusability of the catalyst. Comparing the conversion data, the treated catalyst performs better than the untreated one in first three cycles but falls behind in the fourth cycle surprisingly. This suggests that although thermal treatment can quickly recover the catalytic activity by removing other agents, it will gradually make the adsorption effect weak and finally cause them to drop off from the supports. The selectivity of both the treated and untreated catalyst showed a decline somewhat, which may be ascribed to the absorption of byproducts on the catalyst or the catalyst running off on separation. The byproducts hampered the effective contact between the catalyst and reactants, which also resulted in a lower catalytic activity.

Acknowledgements

We thank the NSAF and NSFC (No: 11076017) of China and Scientific Innovation Program of Jiangsu Province (No: CXZZ11_0264) for support of this research.

Notes and references

1 G. A. Olah, S. J. Kuhn, S. H. Flood and J. C. Evans, *J. Am. Chem. Soc.*, 1962, **84**, 3687.
2 G. A. Olah and S. J. Kuhn, *J. Am. Chem. Soc.*, 1962, **84**, 3684.
3 G. A. Olah, R. Malhotra and S. C. Narang, *Nitration, Methods and Mechanisms*, VCH, New York, 1989.
4 K. Schofield, *Aromatic Nitration*, Cambridge University Press, Cambridge, 1980.
5 T. Okuhara, N. Mizuno and M. Misono, *Adv. Catal*, Academic Press, London, 1996.
6 C. L. Hill and C. M. Prosser-McCartha, *Coord. Chem. Rev.*, 1995, **143**, 407.
7 Y. H. Guo, K. X. Li, X. D. Yu and J. H. Clark, *Appl. Catal., B*, 2008, **81**, 182.
8 S. M. Kumbar and S. B. Halligudi, *Catal. Commun.*, 2007, **8**, 800.
9 S. Gong, L. Liu, Q. Cui and J. Ding, *J. Hazard. Mater.*, 2010, **178**, 404.
10 A. S. Khder and A. I. Ahmed, *Appl. Catal., A*, 2009, **354**, 153.
11 R. J. Kalbasi, M. Ghiaci and A. R. Massah, *Appl. Catal., A*, 2009, **353**, 1.
12 H. Sato, K. Nagai, H. Yoshioka and Y. Nagaoka, *Appl. Catal., A*, 1998, **175**, 201.
13 H. Sato, K. Nagai, H. Yoshioka and Y. Nagaoka, *Appl. Catal., A*, 1998, **175**, 209.
14 M. M. Heravi, T. Benmorad, K. Bakhtiari, F. F. Bamoharram and H. H. Oskooie, *J. Mol. Catal. A: Chem.*, 2007, **264**, 318.
15 A. S. Kumar and P. S. Prasad, *Catal. Commun.*, 2012, **18**, 37.
16 H. Lv, J. Gao, Z. Jiang, Y. Yang, B. Song and C. Li, *Chem. Commun.*, 2007, **13**, 150.
17 C. Li, Z. Jiang, J. Gao, Y. Yang, S. Wang, F. Tian, F. Sun, X. Sun, P. Ying and C. Han, *Chem.–Eur. J.*, 2004, **10**, 2277.
18 H. Lv, J. Gao, Z. Jiang, F. Jing, Y. Yang, S. Wang and C. Li, *J. Catal.*, 2006, **239**, 369.
19 J. Zhang, A. Wang, X. Li and X. Ma, *J. Catal.*, 2011, **279**, 269–275.
20 G. Ranga Rao, T. Rajkumar and B. Varghese, *Solid State Sci.*, 2009, **11**, 36.
21 W. Wu, W. Li, B. Han, Z. Zhang, T. Jiang and Z. Liu, *Green Chem.*, 2005, **7**, 701.
22 G. Li, C. Salim and H. Hinode, *Solid State Sci.*, 2008, **10**, 121.
23 S. T. Yu and F. S. Liu, *Solid Acid Fine Chemicals*, Chemical Industry Press, Beijing, 2005.